Int J Clin Exp Pathol 2017;10(1):306-313
www.ijcep.com /ISSN:1936-2625/IJCEP0040689

Original Article

Neuroradiological findings and clinical features for diagnosis of cerebellar oligodendroglioma: retrospective study of 7 cases

Ruiping Zheng, Yong Zhang, Jingliang Cheng, Chunxiao Bu, Yanliang Li, Anke Dong, Ya Li, Chendi Zhu

MRI Division, The First Affiliated Hospital of Zhengzhou University, Zhengzhou, Henan, China

Received September 26, 2016; Accepted November 11, 2016; Epub January 1, 2017; Published January 15, 2017

Abstract: Objectives: Oligodendroglioma (OD) is the tumors originating from brain oligodendrocytes. Here we aimed to improve diagnosis by analyzing neuroradiological and clinical features of ODs. Methods: We reviewed the clinical records of magnetic resonance imaging (MRI) of seven patients with pathologically proven cerebellar ODs (n = 5) or vermian ODs (n = 2). The ADC ratios and magnetic resonance spectroscopy (MRS) was obtained and analyzed. Results: There were 4 patients (57.1%) with OD, and 3 patients (42.9%) with AOD. The manifestations of the 7 patients included dizziness (n = 3), nausea and vomiting (n = 5), headaches (n = 5), and ataxia (n = 5). The locations of OD were in cerebellar hemispheres (n = 5) or in cerebellar vermis (n = 2). The MRI suggested that lesions of seven patients were hypointense in T1WI, while five were obvious hyperintense in T2WI and 2 lesions with mixed hyperintense. And 3 cases had solid mass, and 4 with cystic necrosis. Moreover remarkable edema was revealed in 4 lesions and 3 with no edema. After injection of Gd-DTPA, all lesions (n = 7) enhanced vividly. On DWI, there were 3 lesions with homogeneously hypointense and 4 with iso-hypointense. The ratios of ODs and AODs were 1.753±0.784 and 1.660±0.551 respectively. There were 4 lesions with hypointense or iso-hypointense and 3 lesions with hyperintense or iso-hyperintense. There were four lesions with obvious edema in most adjacent area. The MRS of ODs revealed increased Cho and reduced NAA. Conclusions: The ADC, MRS, calcification and contrast enhancement can help to differentiate ODs from other gliomas.

Keywords: Oligodendroglioma, anaplastic oligodendroglioma, magnetic resonance imaging

Introduction

Oligodendroglioma (OD) is the tumors originating from brain oligodendrocytes which are epithelial tissue tumors typically graded as grade II (oligodendroglioma, OD) and grade III (anaplastic oligodendroglioma, AOD) according to the 2007 World Health Organization (WHO) classification of tumors in central nervous system [1]. ODs and AODs allocate 1.7% and 0.5% of brain tumors respectively [2]. moreover ODs account for no more than 4% of the primary central nervous system tumors and 5%-18% of all gliomas [3, 4]. Now the preferred treatment of ODs is surgical resection which is still under discussion [5, 6]. The overwhelming majority of these lesions are situated in the supratentorial compartment, and only several cases within fratentorial ODs published in the past few years. Most ODs arise in white matter of cerebral hemispheres, predominantly in the frontal lobes, somewhat more frequently in males and with the peak incidence in the 4th and 6th decade of life [7-9]. Although ODs are well-differentiated and have a more indolent clinical history and significantly prolonged survival compared with their astrocytic counterparts, Lee et al. viewed that infratentorial ODs may be more malignant than supratentorial ODs [10]. Therefore early diagnosis of ODs is important to formulating an appropriate treatment. Due to the rarity of this tumor, a systematic analysis of MR imaging features of ODs has not yet been performed. To determine specific diagnostic features, here we reported on imaging characteristics of 7 cases that were confirmed by pathologists.

Materials and methods

Patients

Approval of institutional review board was obtained and the requirement for patient consent

was acquired for this retrospective study in which 7 patients with surgical and histological evidences of ODs were performed in our hospital from June 2012 to August 2015. There are three men and four women ranging from 3 to 66 years old.

Magnetic resonance imaging

MRI examinations were performed with 1.5-T and 3.0-T units (produced by Verio, Siemens; GE750, GE Medical Systems) on all 7 patients. Transverse and sagittal T1-weighted spin echo images were obtained at the following parameters: repetition time msec/echo time msec, 7500/114; field of view, 229 mm × 229 mm; section, 5 mm; matrix, 288 × 288 or 512 × 512. Transverse T2-weighted images were obtained at the following parameters: 6000/125; field of view, 240 mm × 240 mm; section thickness, 5 mm; matrix, 384 × 384 or 512 × 512; acquisition time. Transverse fluid-attenuated inversion-recovery sequences (6500/85; field of view, 240 mm × 240 mm or 512 × 512; section thickness, 5 mm) and contrast-enhanced transverse, sagittal, and/or coronal T1-weighted spin echo sequences (240/2.5; field of view, 229 mm × 229 mm; section thickness, 5 mm) were performed after administration of gadolinium diethylenetriaminepentaacetic acid (Gd-DTPA, produced by Consun Pharmaceutical Co., Ltd, Guangzhou, China; 0.2 mmol per kilogram of body weight).

The degree of edema was judged as follows: a mean diameter of peripheral edema with less than 10 mm was graded as mild edema, a mean diameter of 11-20 mm as moderate edema, and a mean diameter of more than 20 mm as marked edema [11].

DWI and measurement of ADC values

Diffusion weight imaging (DWI) was performed a spin echo sequence with b = 0 and b = 1,000 s/mm^2 as well as generated by the application of diffusion gradients in three orthogonal directions. ADC maps were generated with a monoexponential fit on a voxel-to-voxel basis for all imaging planes. With the using of a DICOM viewer (RadiAnt DICOM Viewer, Medixant, Poznan, Poland), the measurements of the radiology was achieved. The ADC values were obtained from the solid portions in three consecutive slices of tumor tissues, in which the necrotic or presumably hemorrhagic foci (hyperintense on conventional T1 weighted images) were excluded. The ADC value of the normal cerebellum was recorded by using three regions of interest (ROIs). The ROI placement in normal cerebellum was orientated as far away as possible from the tumor with exclusion of vasogenic edema. Calculate the mean of minimum ADC values obtained from the three ROIs. The ADC ratio was calculated by dividing the minimum tumor ADC to the minimum ADC of normal cerebellum.

Magnetic resonance spectroscopy

For MRS, spectral and metabolite maps for each slice along the third dimension were extracted by FuncTool Display. Within the obtained volume of interest (VOI), separate voxels were individually placed in different parts of tumor. The metabolite peaks had included N-acetylaspartate (NAA) at 2.02 ppm; choline-containing compounds (Cho) at 3.22 ppm; (phospho-) creatine (Cr) at 3.01 ppm; and lipid (Lip) at 1.30 ppm. Metabolite ratios (Cho/Cr) were calculated from the metabolite maps by using the relevant software.

Imaging analysis

All MRI images were retrospectively reviewed by two experienced neuroradiologists. The images were specifically evaluated with lesion size, shape, attenuation and signal intensity, characteristics of enhancement and peripheral edema. In addition, clinical data, such as age, sex, and symptoms, were reviewed. All OD patients confirmed by operation and biopsy were given surgical resection or treated with additional radiotherapy based on the pathological results.

Statistical analysis

The data were treated with SPSS 21.0 statistical analysis software. The measurement data obeying a normal distribution were showed as $\bar{X}\pm s$. For non-normal measurement data, median and interquartile range was used to measure the central and discrete tendency. To compare differences among groups, the measurement data was using t-test and variance analysis, and the enumeration data using rank sum test. When p is less than 0.05, the differences were statistically significant.

Results

Clinical features

Patients' characteristics and clinical characteristics are summarized in Supplementary Table

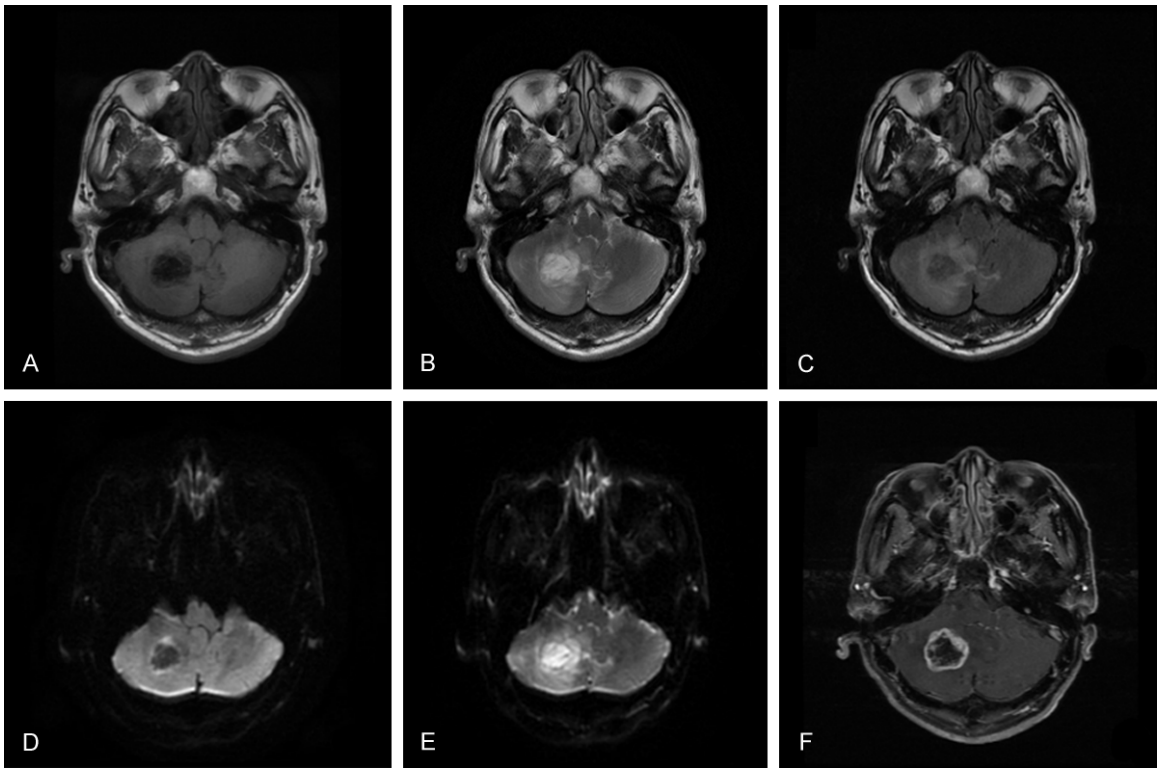

Figure 1. Oligodendroglioma in right cerebellar hemisphere. A. The lesion presents as obviously hypointense on pre-contrast axial T1WI; B. Distinctly hyperintense on axial T2WI; C. Hyperintense on FLAIR sequence with hypointense in the cystic-necrotic areas; D. Axial DWI MR shows no obviously diffusion restriction of the lesion; E. The ADC map presents visibly hypointensity of the lesion and hyperintense of the cystic-necrotic areas; F. Post-contrast axial T1WI shows marked enhancement of the lesion, without enhancement in the cystic-necrotic area.

1. This study comprised 7 patients (3 males and 4 females), ranging from 3 to 66 years old. There are several initial symptoms, dizziness (*n* = 3), nausea and vomiting (*n* = 5), headaches (*n* = 5), ataxia (*n* = 5), et al. The duration of clinical symptoms had varied from a few days to two months.

MR imaging features

In our cohort, the locations of OD were cerebellar hemispheres (n = 5) (**Figure 1**) and cerebellar vermis (n = 2) (**Figure 2**). The maximum diameter of the lesions ranged from 1.7 cm to 4.0 cm (with an average of 3.0±0.8 cm). On T1WI, all lesions appeared to be hypointense. However, on T2WI, 5 lesions appeared to be vividly hyperintense, while the other 2 lesions appeared to be mixed hyperintense. Otherwise, there are 3 cases with solid mass and 4 cases with cystic necrosis. Among 7 lesions, the remarkable edemas were revealed in 4 lesions (57.14%). After the injection of Gd-DTPA, all lesions (n = 7) enhanced vividly, and 1 of these 7 lesions presented as heterogeneous enhancement. The FLAIR revealed that there were 4 lesions (57.14%) with obvious hypointense or iso-hypointense and 3 lesions (42.86%) with hyperintense or iso-hyperintense. There were 4 lesions with severe edema in most adjacent area of tumor tissue and 3 lesions with no edema. The classification of tumor was divided into four based on time-intensity curve (TIC): In type A, the time of peak (*T* peak) is longer than 120 s. In type B, the *T* peak is equal or shorter than 120 s and the washout ratio (WR) is equal or greater than 30%. In type C, *T* peak is equal or shorter than 120 s and the WR was less than 30%. In type D, the TIC was flat [12]. All of these 7 patients were type A (**Figure 3**).

DWI MR images

In the high (b = 1000 s/mm^2) b-value DWI images, 3 patients appeared as homogeneously hypointense, while 4 patients showed iso-hypointense with mildly restricted diffusion of protons, a characteristic of cytotoxic edema.

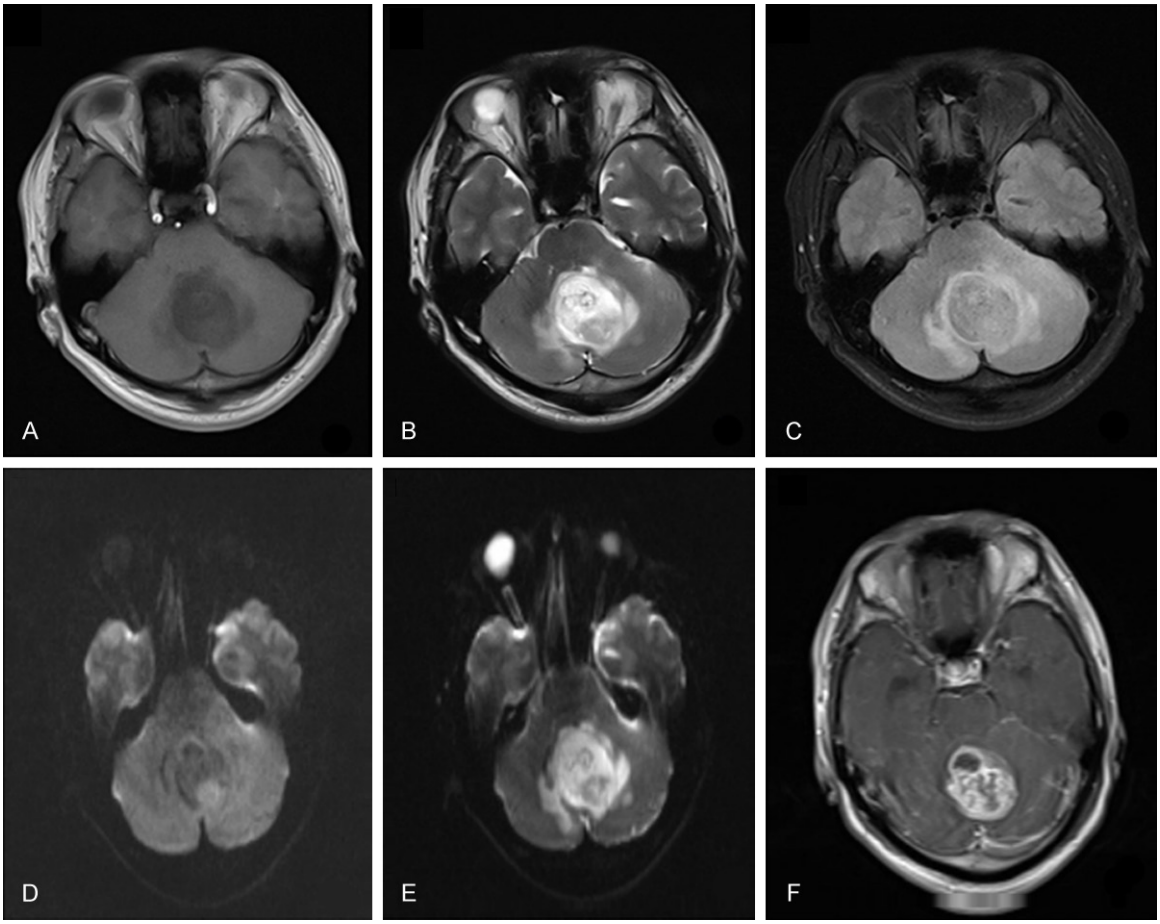

Figure 2. Oligodendroglioma incerebellar vermis. A. The lesion presents as obviously hypointense on pre-contrast axial T1WI; B. Distinctly inhomogeneous hyperintense on axial T2WI with distinctly peritumoral edema; C. Iso-tohyperintense on FLAIR sequence; D. Axial DWI MR shows diffusion restriction; E. The ADC map presents visibly hyperintensity; F. Post-contrast axial T1WI shows marked enhancement.

The ADC values of 7 patients were calculated, the mean ADC_{min} values of ODs and aplastic ODs were (0.966±0.496) × 10^{-3} mm^2/s and (1.461±1.177) × 10^{-3} mm^2/s respectively. Moreover, ADC maps displayed heterogeneous hypointensity or isointensity. Compared with the normal cerebrum, the mean tumor ADC_{min} ratio values were 1.753±0.784 and 1.660±0.551 respectively (Supplementary Table 1), moreover a variability of ADC ratio values among lesions was observed even within individual patients, ranging from 0.770 to 2.661.

Magnetic resonance spectroscopy features

The MRS exhibited an elevated Cho peak and Cho/Cr ratios, and a reduced NAA peak and NAA/Cr ratios without a lactate peak. Here the MRS of one patient is displayed (**Figure 4**).

Pathological and immunohistochemical features of ODs

All patients were accepted surgical resection; the gross pathology of the ODs was characterized by nodular, well-circumscribed and gray soft mass. Strong diffuse nuclear staining of p53 was present in only 2 cases. Otherwise as shown in the immunohistochemical result, all cases expressed GFAP, Ki-67 and S-100 (**Figure 5**), while Oligo-2 was noted in 7 patients.

Discussion

In our knowledge ODs are less prevalent than astrocytomas and have a more chronic clinical history and prolonged survival compared with astrocytic tumors of the same grade. However, they seem to be more common than previously thought [13]. Although ODs have unique patho-

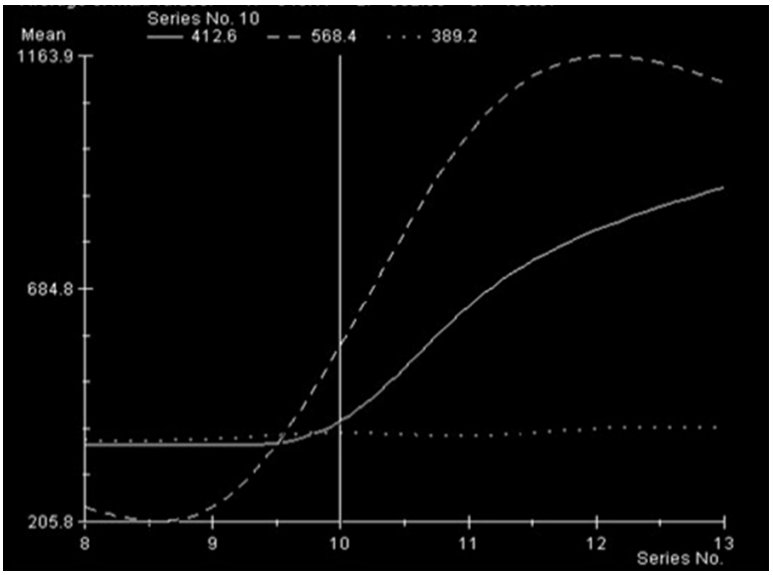

Figure 3. The TIC of a type A oligodendroglioma in the left cerebellar hemispheres.

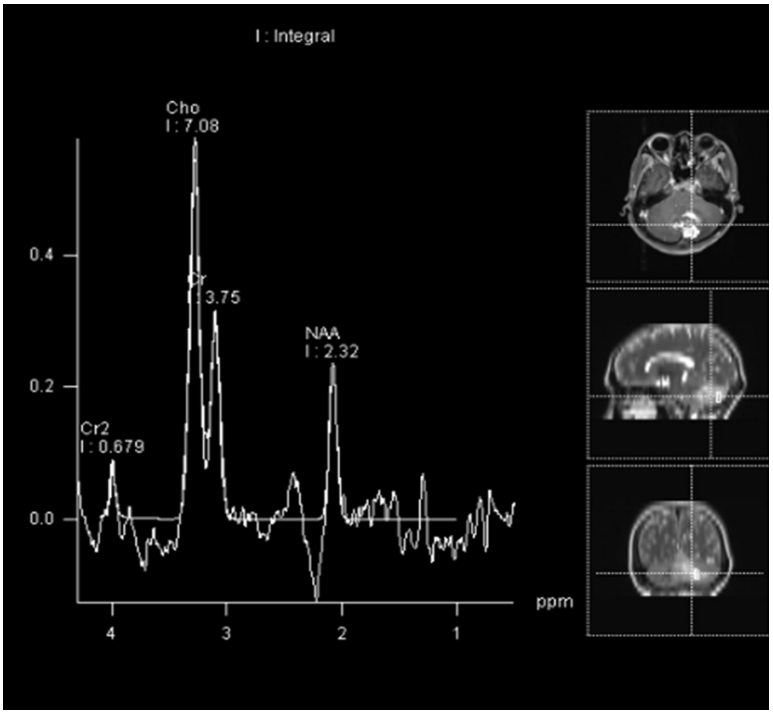

Figure 4. MRS image of a patient. MRS image exhibits an elevated Cho peak, and reduced NAA. The absence of a lactate/lipid peak is also noted.

logical and clinical characteristics, it is difficult to distinguish them from other types of gliomas because of the atypical clinical symptoms of ODs and differences according to locations of tumor growth [14]. For instance, patients exhibiting generalized tonic-clonicseizures were proved to be more often to have the greatest lesion in mesial frontal regions, while the ODs of patients with partial seizures were load more caudolaterally in orbitofrontal and temporal lobes, which indicates that the location of the lesion is a major factor of seizure's type. In most series, seizure has been the most common presenting symptom, ranging in incidence from 35% to 85% [15]. Other presenting symptoms include headaches, vertigo, nausea, mental status changes, visual complaints, and/or localized weakness [15]. Classically, it has been observed that patients with ODs often experience symptoms (usually seizures) for a number of years prior before their diagnosis, which was definitively made after an apoplectic event such as peritumoral haemorrhage. The clinical course of OD in the posterior cranial fossa is relatively chronic with longstanding symptoms [16, 17]. ODs account for up to 33% of all gliomas in adult which rarely arise in the infratentorial compartment [18]. Thus, how to diagnose posterior fossa ODs is still a strong challenge for the clinicians.

To date, only very limited MR imaging data of OD in cerebellar hemisphere are available in scattered case reports. On conventional MR imaging scans, the solid lesions with little or no necrosis appear as obviously hypointense on T1WI, and distinctly hypertense on T2WI. Our result in which necrosis was observed in four patients with heterogeneous hyperintense in internal architecture on T2WI supports this assessment. Cystic degeneration and haemorrhage may occur, but not frequent.

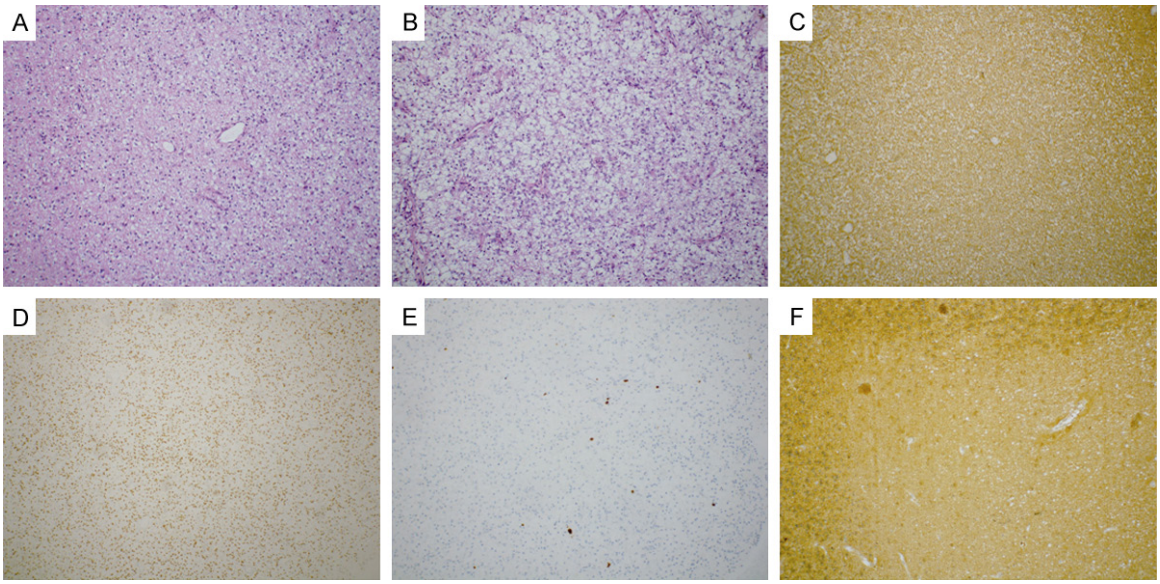

Figure 5. Pathological and immunohistochemical images of ODs. (A and B) Photomicrograph showed small round cells with nuclei, surrounded by a halo, demonstrating a characteristic "fried egg" appearance. (C-F) Immunohistochemistry showed that the tumor cells were positive for oligodendroglioma marker GFAP (C), Oligio-2 (D), Ki-67 (E) and NSE (F) (C. Chaematoxylin-and eosin-stained sections at 200 ×; E. Haematoxylin-and eosin-stained sections at 100 ×).

Peritumoural edema is also not common. These features tend to point towards anaplastic degeneration of the tumor [15, 19]. ODs have a better prognosis. Nevertheless, these tumors ineluctably undergo anaplastic transformation, which is associated with a poor prognosis [20]. In our cohort, 4 of 7 patients show peritumoural edema, which shows markedly hyperintense on T2 Flair. Among the 4 patients, 3 lesions were classified as AODs. Mass effects are usually minimal or absent, despite of the size of the tumor [15]. Therefore, peritumoural edema and mass effect can be used to identify OD from other gliomas. Calcification is another hallmark feature of OD [9, 21]. Calcification often presents a coarse appearance. However, punctate or linear calcification may also occur. Calcifications were seen more frequently in AODs rather than ODs [22].

ODs have been reported to show frequent postcontrast enhancement on MR imaging [23]. Most studies have reported that 50%-60% of ODs exhibit contrast enhancement which is associated with the malignant degree of tumor [24, 25]. Among the enhancing tumors, a greater number of AODs show enhancement as opposed to ODs, and this difference in enhancement is statistically significant. Our result shows that all patients exhibit obviously enhanced, and one of them presents distinctly heterogeneous enhancement. In our study, 4 patients had undergone dynamic MR imaging, and all of them were type A of TIC curve. This was considered to be gradual enhancement, which showed that the mechanism of enhancement was associated with the damage of blood brain barrier.

ADC value derived from diffusion MR imaging provides a measurement of the movement of water molecules within tissue microstructures, so ADC may provide information regarding tumor cellularity and the biology of brain tumors. Previous studies used ADC maps on DWI to determine the tumor grade [26, 27]. An association between tumor cellularity and ADC has been proposed in the study of Kono [27]. In our study, the mean ADC_{min} ratio value of ODs is 1.753±0.784, and the AOD is 1.660±0.551. Khalid L, et al. Moreover AODs are reported to have low ADC values compared with ODs with a threshold value of 0.925 × 10^3 mm^2/s [22], likely due to water restriction within these tumors to a high nucleus-to-cytoplasm ratio, hypercellularity and higher ADC values in low-grade tumors [28]. Our results support this by demonstrating a statistical difference between ADC values for grade III and grade II tumors.

MR spectroscopy is used to measure regional variations in neurochemistry and the concentration of various brain metabolites. Smits M reported that the typical spectrum of ODs shows moderately elevated Cho, which correlates with membrane biosynthesis by proliferating cells, and decreased NAA, which indicates loss of neuronal integrity due to tumor cell infiltration, without a lactate peak, and our observations on MRS were similar [19, 29]. Furthermore, as previously reported, Cho/Cr and Cho/NAA ratios were significantly higher in grade III compared with grade II gliomas tumors [30-32]. Apart from it, the absence of a lactate/lipid peak can also distinguish ODs from AODs.

Conclusion

The ADC, MRS, calcification and contrast enhancement can help to differentiate ODs from other gliomas. Furthermore, these imaging characteristics assist in predicting the grade of ODs and help direct biopsy sites and predict prognosis.

Disclosure of conflict of interest

None.

Address correspondence to: Yong Zhang, MRI Division, The First Affiliated Hospital of Zhengzhou University, Zhengzhou 450052, Henan, China. Tel: +86-0371-55966339; Fax: +86-0371-67077303; E-mail: yongzhang11223@sohu.com

References

[1] Louis DN, Ohgaki H, Wiestler OD, Cavenee WK, Burger PC, Jouvet A, Scheithauer BW, Kleihues P. The 2007 WHO classification of tumours of the central nervous system. Acta Neuropathol 2007; 114: 97-109.

[2] Hodges SD, Malafronte P, Gilhooly J, Skinner W, Carter C, Theeler BJ. Rare brainstem oligodendroglioma in an adult patient: presentation, molecular characteristics and treatment response. J Neurol Sci 2015; 355: 209-10.

[3] Chawla S, Krejza J, Vossough A, Zhang Y, Kapoor GS, Wang S, O'Rourke DM, Melhem ER, Poptani H. Differentiation between oligodendroglioma genotypes using dynamic susceptibility contrast perfusion-weighted imaging and proton MR spectroscopy. AJNR Am J Neuroradiol 2013; 34: 1542-9.

[4] Wesseling P, van den Bent M, Perry A. Oligodendroglioma: pathology, molecular mechanisms and markers. Acta Neuropathol 2015; 129: 809-27.

[5] Aghi MK, Nahed BV, Sloan AE, Ryken TC, Kalkanis SN, Olson JJ. The role of surgery in the management of patients with diffuse low grade glioma: a systematic review and evidence-based clinical practice guideline. J Neurooncol 2015; 125: 503-30.

[6] Atalay T, Ak H, Celik B, Gulsen I, Seckin H, Tanik N, Albayrak SB, Bavbek M. Prognostic factors in oligodendrogliomas: a clinical study of twenty-five consecutive patients. Asian Pac J Cancer Prev 2015; 16: 5319-23.

[7] Arevalo-Perez J, Kebede AA, Peck KK, Diamond E, Holodny AI, Rosenblum M, Rubel J, Gaal J, Hatzoglou V. Dynamic contrast-enhanced MRI in low-grade versus anaplastic oligodendrogliomas. J Neuroimaging 2015; 26: 366-71.

[8] Lamis FC, de Paiva Neto MA, Stavale JN, Cavalheiro S. Low-grade oligodendroglioma of the pineal region: case report. J Neurol Surg Rep 2015; 76: e55-8.

[9] Zulfiqar M, Dumrongpisutikul N, Intrapiromkul J, Yousem DM. Detection of intratumoral calcification in oligodendrogliomas by susceptibility-weighted MR imaging. AJNR Am J Neuroradiol 2012; 33: 858-64.

[10] Lee IH, Kim ST, Suh YL, Kim HJ, Kim KH, Jeon P, Byun HS. Infratentorial oligodendrogliomas: imaging findings in six patients. Acta Radiol 2010; 51: 213-7.

[11] Zhang D, Hu LB, Henning TD, Ravarani EM, Zou LG, Feng XY, Wang WX, Wen L. MRI findings of primary CNS lymphoma in 26 immunocompetent patients. Korean J Radiol 2010; 11: 269-77.

[12] Yabuuchi H, Fukuya T, Tajima T, Hachitanda Y, Tomita K, Koga M. Salivary gland tumors: diagnostic value of gadolinium-enhanced dynamic MR imaging with histopathologic correlation. Radiology 2003; 226: 345-54.

[13] Paleologos NA. Oligodendroglioma. Curr Treat Options Neurol 2001; 3: 59-66.

[14] Wieshmann UC, Milinis K, Paniker J, Das K, Jenkinson MD, Brodbelt A, Crooks D, Keller SS. The role of the corpus callosum in seizure spread: MRI lesion mapping in oligodendrogliomas. Epilepsy Res 2015; 109: 126-33.

[15] Ouni FE, Gaha M, Moulahi H, Daadoucha A, Krifa H, Tlili K. Infratentorial oligodendroglioma in a child: a case report and review of the literature. Turk Neurosurg 2012; 22: 461-4.

[16] Jenkinson MD, du Plessis DG, Smith TS, Joyce KA, Warnke PC, Walker C. Histological growth patterns and genotype in oligodendroglial tumours: correlation with MRI features. Brain 2006; 129: 1884-91.

[17] Nadkarni TD, Menon RK, Desai KI, Goel AH. Cerebellar oligodendroglioma in a young adult. J Clin Neurosci 2005; 12: 837-8.

[18] Engelhard HH, Stelea A, Cochran EJ. Oligodendroglioma: pathology and molecular biolo-

gy. Surg Neurol 2002; 58: 111-7; discussion 117.
[19] Smits M. Imaging of oligodendroglioma. Br J Radiol 2016; 89: 20150857.
[20] Bourdillon P, Hlaihel C, Guyotat J, Guillotton L, Honnorat J, Ducray F, Cotton F. Prediction of anaplastic transformation in low-grade oligodendrogliomas based on magnetic resonance spectroscopy and 1p/19q codeletion status. J Neurooncol 2015; 122: 529-37.
[21] Wagner MW, Poretti A, Huisman TA, Bosemani T. Conventional and advanced (DTI/SWI) neuroimaging findings in pediatric oligodendroglioma. Childs Nerv Syst 2015; 31: 885-91.
[22] Khalid L, Carone M, Dumrongpisutikul N, Intrapiromkul J, Bonekamp D, Barker PB, Yousem DM. Imaging characteristics of oligodendrogliomas that predict grade. AJNR Am J Neuroradiol 2012; 33: 852-7.
[23] Lee YY, Van Tassel P. Intracranial oligodendrogliomas: imaging findings in 35 untreated cases. AJR Am J Roentgenol 1989; 152: 361-9.
[24] Reiche W, Grunwald I, Hermann K, Deinzer M, Reith W. Oligodendrogliomas. Acta Radiol 2002; 43: 474-82.
[25] White ML, Zhang Y, Kirby P, Ryken TC. Can tumor contrast enhancement be used as a criterion for differentiating tumor grades of oligodendrogliomas? AJNR Am J Neuroradiol 2005; 26: 784-90.
[26] Arvinda HR, Kesavadas C, Sarma PS, Thomas B, Radhakrishnan VV, Gupta AK, Kapilamoorthy TR, Nair S. Glioma grading: sensitivity, specificity, positive and negative predictive values of diffusion and perfusion imaging. J Neurooncol 2009; 94: 87-96.
[27] Kono K, Inoue Y, Nakayama K, Shakudo M, Morino M, Ohata K, Wakasa K, Yamada R. The role of diffusion-weighted imaging in patients with brain tumors. AJNR Am J Neuroradiol 2001; 22: 1081-8.
[28] Sadeghi N, Camby I, Goldman S, Gabius HJ, Baleriaux D, Salmon I, Decaesteckere C, Kiss R, Metens T. Effect of hydrophilic components of the extracellular matrix on quantifiable diffusion-weighted imaging of human gliomas: preliminary results of correlating apparent diffusion coefficient values and hyaluronan expression level. AJR Am J Roentgenol 2003; 181: 235-41.
[29] A O. Osborns brain imaging pathology anatomy. Salt Lake City, UT: Amirsys, Inc 2012.
[30] Spampinato MV, Smith JK, Kwock L, Ewend M, Grimme JD, Camacho DL, Castillo M. Cerebral blood volume measurements and proton MR spectroscopy in grading of oligodendroglial tumors. AJR Am J Roentgenol 2007; 188: 204-12.
[31] Stadlbauer A, Gruber S, Nimsky C, Fahlbusch R, Hammen T, Buslei R, Tomandl B, Moser E, Ganslandt O. Preoperative grading of gliomas by using metabolite quantification with high-spatial-resolution proton MR spectroscopic imaging. Radiology 2006; 238: 958-69.
[32] Fellah S, Caudal D, De Paula AM, Dory-Lautrec P, Figarella-Branger D, Chinot O, Metellus P, Cozzone PJ, Confort-Gouny S, Ghattas B, Callot V, Girard N. Multimodal MR imaging (diffusion, perfusion, and spectroscopy): is it possible to distinguish oligodendroglial tumor grade and 1p/19q codeletion in the pretherapeutic diagnosis? AJNR Am J Neuroradiol 2013; 34: 1326-33.

Supplementary Table 1. Case Summary of Oligodendrogliomas

Case No.	Age/ Sex	WHO grade	Location	Type	Edema	ADC values		Conventional MR imaging scans					Enhance
						Tumor (mm^2/s)	Contralateral normal cerebellum (mm^2/s)	rADC min	T1WI	T2WI	T2 flair	DWI	
1	3/m	II	Left cerebellar hemispheres	Cystic	No	1.246	0.640	1.947	Low	High	Low	Iso-low	Obvious
2	7/f	II	Cerebellar vermis	Cystic	No	0.314	0.408	0.770	Low	High	Iso-low	Iso-	Obvious
3	30/m	II	Left cerebellar hemispheres	Solid	Yes	0.864	0.529	1.633	Low	High	Iso-high	Iso-low	Obvious
4	35/f	II	Right cerebellar hemispheres	Cystic	No	1.440	0.541	2.662	Low	Mixed high	Low	Low	Heterogeneous
5	50/f	III	Right cerebellar hemispheres	Solid	Yes	0.900	0.609	1.478	Low	Iso-high	High	Iso-	Obvious
6	50/f	III	Cerebellar vermis	Solid	Yes	0.670	0.551	1.216	Low	High	High	Low	Obvious
7	66/m	III	Right cerebellar hemispheres	Cystic	Yes	2.813	1.237	2.274	Low	High	Low	Low	Obvious